Journal of
Computational and Theoretical Nanoscience
Vol. 6, 1–8, 2009

Analytical Formulation of Stress Distribution in Cellulose Nanocomposites

K. Momeni* and R. S. Yassar

Department of Mechanical Engineering-Engineering Mechanics, Michigan Technological University, US

Cellulose nanofibers are known to possess aspect ratios larger than 200 and mechanical properties comparable to carbon nanotubes. Combined with other significant properties including low cost, low density, and biocompatibility, cellulose nanofibers are an attractive reinforcement material for nanocomposites. The load transfer between embedded fibers and matrix play a major role in designing nanocomposites with ultimate mechanical properties. In this work, we studied a general case where a simple axial loading exists along the axis of a cellulose fiber embedded in a polymer matrix. Then analytical relation between the applied load, the longitudinal stress along the fiber, and shear stresses along the interface of fiber and matrix was derived. It is shown that the maximum longitudinal stress occurs at the middle of the fiber, while maximum shear stress occurs at the extreme ends. Also, it is shown that the shear stress along the cellulose fibers can be approximated as a linear function of applied load. The derived relationships are useful for design of cellulose-based nanocomposites with enhanced mechanical properties.

Keywords: Analytical Modeling, Nano-Structures, Stress Transfer, Cellulose.

RESEARCH ARTICLE

1. INTRODUCTION

Cellulose nanofiber consists of highly crystalline rod-like particles which have a high aspect ratio (above 200)[1] and large surface area (about 150 m^2/g).[2] They can be found abundantly in nature and can be obtained from different sources such as plants and living organisms.[3] Furthermore, cellulose is a low cost, low density and renewable material with mechanical properties comparable to carbon nanotubes.[4] The main reason for such superior properties of nanomaterials reinforcement is their size and structure. While they have high surface area and high aspect ratio due to their small size, their defect free structure is the main source of their superior mechanical properties.[5] These unique properties of cellulose nanofibers are attractive for enhancing the properties of different polymers,[6] and in particular, bio-based polymers due to biocompatibility and biodegradability of cellulose materials.[7]

Composite materials reinforced with cellulose nanofibers show substantial improvement in tensile modulus and yield strength in comparison to unfilled polymers.[8] Lapa et al.[9] have reported a 70% increase in stress at failure and 100% increase in the elastic modulus of nitrile rubber when it was filled with 20 phr of cellulose nanocrystals. Choi and Simonsen[10] showed that with 5% addition of cellulose nanofibers to carboxymethyl cellulose the tensile strength, elastic modulus, and toughness of the nanocomposite could improve by 17%, 60% and 60% respectively. Auad et al.[11] reported 53% increase in elastic modulus in 1 wt% cellulose nanofiber reinforced polyurethane composite samples. Noorani et al.[12] observed that the highest overall increase of tensile modulus with the addition of 7 wt% cellulose nanofiber. It was reported that the tensile modulus decreases for higher volume fractions of cellulose nanofiber due to the agglomeration of cellulose nanofibers. Zimmermann et al.[13, 14] conducted a series of nanoindentation tests and reported that the addition of the hydroxypropyl cellulose (HPC) fibrils increased the elastic modulus up to three-fold and the tensile strength up to five-fold compared to the raw polymer. A homogeneous cellulose distribution as well as a rigid network resulting from hydrogen bonds between adjacent and overlapping fibrils (percolating network) has been proposed to explain the improved mechanical behavior of reinforced composites.[13, 15, 16]

In fiber-reinforced polymer composites, it is widely accepted that the performance of a composite as a structural material depends mainly on the quality of the stress transfer in the interface.[17] The nature of the interface within a thickness less than 5 μm is rarely reported in the literature because experimental means of unequivocally establishing the interface properties are lacking.

*Author to whom correspondence should be addressed.

Lee et al.[18] investigated the mechanical properties in the interface in cellulose fiber-reinforced polypropylene composites using nanoindentation. However, they could not obtain an accurate estimation of the mechanical properties due to the effect of neighboring material properties smaller than the indenter size.

The main mechanism for strong binding between cellulose nanocrystal and polymer can be mechanical interlocking of the nanocrystals and polymer molecules, covalent chemical bonding and non-covalent bonding like Van der Waals and electrostatic forces. The relative contribution of the three factors, i.e., the dominant mechanism, to the bonding is unknown. It is also unclear, whether the bonding mechanisms depend on the cellulose nanocrystal-polymer system and/or functionalization of the polymer. Qian et al.[19] discovered that surface forces like friction and adhesion are the main factors governing the strength of the interface in carbon nanotube reinforced polymers. Frictional forces could be a crucial factor in determining the behavior of the interface. This means that even if the cellulose nanocrystal/polymer bond fails, the frictional forces will prevent slipping of the nanocrystal and ensure good load transfer between polymer and cellulose nanocrystal. It is evident that a better understanding of interface nanomechanics and the correlation with mechanical properties of cellulose nanocomposite can be beneficial for the optimal design of these materials.

In general, the composite materials fail when one of its constitutive components or the interface bonding between them, fails.[20] For the case of cellulose the interfacial stresses play a major role compared to the other reinforcement materials. It is due to the fact that while cellulose has a polar surface, polymer matrix has a hydrophilic interface.[21] Therefore a key step in designing composite material is finding the magnitude of stress which is applied to each component, and also the surface tension at the interface of different phases. In this work stress distribution on the fiber and along the fiber/matrix interface was derived analytically as a function of applied axial load. The mathematical formulation is based on continuum mechanics approach with some simplifying assumptions that are discussed in the next section. For deriving the governing differential equations, three dimensional theory of elasticity is employed. The governing equilibrium equations of an axisymmetric problem in cylindrical coordinate (r, θ, z) is considered. Using kinematical relations, constitutive equations and finally applying boundary conditions in both reinforced and pure matrix parts of the RVE, the governing differential equations are obtained. Solving these differential equations leads to the stress distribution on the fibers.

2. GEOMETRY AND ASSUMPTIONS

The external force was considered to be applied along the longitudinal axis of the cellulose fibers. This is the direction which the cellulose fiber has the maximum reinforcing effect. The corresponding Representative Volume Element (RVE) for this problem is shown in Figure 1. The side views of embedded cellulose fiber in the matrix are shown in Figure 2.

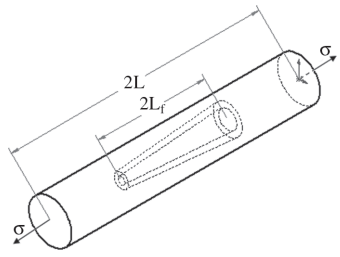

Fig. 1. RVE of a cellulose fiber with length of $2L_f$ embedded in a matrix with length of 2L. The composite is then being subjected to the overall stress of σ along the cylindrical axis.

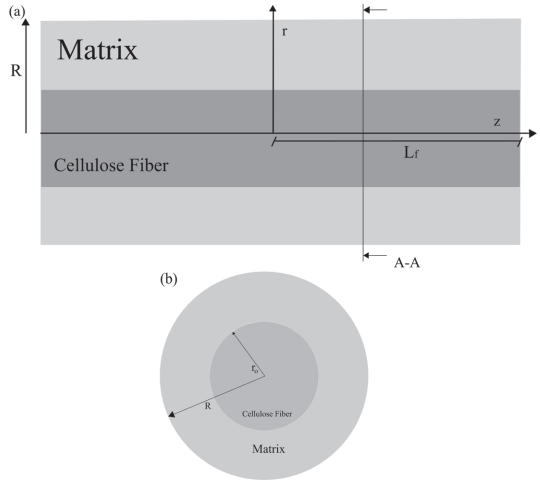

Fig. 2. (a) Side view and (b) cross-sectional view, A-A, of the RVE shown in Figure 1.

The epoxy matrix and cellulose fiber both were considered to be isotropic with perfect interfacing bonding. As it is shown in Figure 1, we assumed the longitudinal length of the RVE and cellulose fiber as 2L and $2L_f$, respectively. Also the applied axial load is transferred to the cellulose fiber via surrounding matrix. Due to the loading configuration it can be concluded that the radial and hoop stresses are much smaller than the axial stresses, i.e., $\sigma_{\theta\theta} + \sigma_{rr} \ll \sigma_{zz}$. In addition, the effect of body forces has been neglected.

3. MODELING AND SOLUTION

The equilibrium equations in absence of body forces, for axisymmetric problem in terms of cylindrical coordinate (r, θ, z) are:[22]

$$\frac{\partial \sigma_{rr}}{\partial r} + \frac{\partial \tau_{rz}}{\partial z} + \frac{\sigma_{rr} - \sigma_{\theta\theta}}{r} = 0 \qquad (1a)$$

$$\frac{\partial \tau_{rz}}{\partial r} + \frac{\partial \sigma_{zz}}{\partial z} + \frac{\tau_{rz}}{r} = 0 \tag{1b}$$

Assuming the u and w as displacement along r and z direction, the geometrical equations for cellulose fiber can be written as:

$$\varepsilon_{rr} = \frac{\partial u}{\partial r} \tag{2a}$$

$$\varepsilon_{\theta\theta} = \frac{u}{r} \tag{2b}$$

$$\varepsilon_{zz} = \frac{\partial w}{\partial z} \tag{2c}$$

$$\gamma_{rz} = \frac{\partial u}{\partial z} + \frac{\partial w}{\partial r} \tag{2d}$$

Assuming cellulose fiber and matrix as elastic materials, the constitutive equations are:

$$\varepsilon_{rr} = \frac{1}{E}[\sigma_{rr} - \nu(\sigma_{\theta\theta} + \sigma_{zz})] \tag{3a}$$

$$\varepsilon_{\theta\theta} = \frac{1}{E}[\sigma_{\theta\theta} - \nu(\sigma_{zz} + \sigma_{rr})] \tag{3b}$$

$$\varepsilon_{zz} = \frac{1}{E}[\sigma_{zz} - \nu(\sigma_{rr} + \sigma_{\theta\theta})] \tag{3c}$$

$$\gamma_{rz} = \frac{\tau_{rz}}{G} \tag{3d}$$

where the other strain components are vanished due to the problem configuration and geometry of applied forces, i.e., axial loading.

In the next step we will define the boundary equations for the above mentioned governing equations. The boundary conditions (4) describe the force balance at the boundaries of the RVE. The Eq. (5) are due to the force balance at the cellulose fiber/matrix interface. According to the type of loading, there is no traction along radial direction on the surface of the RVE, i.e., Eq. (4a). The stress σ is applied on the extremes of the cellulose fiber along its axis of symmetry, which leads to Eq. (4b). In Eq. (4b) $\hat{e}_z$is the unit vector along the z-axis.

$$\begin{cases} T^m|_{r=R} = 0 & (4a) \\ T^m|_{z=\pm L_f} = \pm\sigma\hat{e}_z & (4b) \end{cases}$$

The force balance between the cellulose fiber and matrix along the radial direction and at the extreme ends, leads to following equations.

$$\begin{cases} T^f|_{-L_f<z<L_f, r=r_o} = T^m|_{-L_f<z<L_f, r=r_o} & (5a) \\ T^f|_{z=\pm L_f, 0<r<r_o} = T^m|_{z=\pm L_f, 0<r<r_o} & (5b) \end{cases}$$

3.1. Solution in Reinforced Region

In general, the integration of Eq. (1b) with respect to r from r_i to r_o for a reinforcing cellulose fiber designated by superscript f:

$$\frac{1}{\pi r_o^2}\int_0^{r_o} \frac{\partial \sigma_{zz}^f}{\partial z}(2\pi r)\,dr + \frac{1}{\pi r_o^2}\int_0^{r_o} \frac{1}{r}\frac{\partial}{\partial r}(r\tau_{rz}^f)(2\pi r)\,dr = 0 \tag{6}$$

where the first part of (6) can be defined as an average axial normal stress over the cross section of the cellulose fiber as below:

$$\bar{\sigma}_{zz}^f = \frac{1}{\pi r_o^2}\int_0^{r_o} \sigma_{zz}^f(r,z)\cdot(2\pi r)\,dr \tag{7}$$

Differentiation of (7) with respect to z and using (6) leads to:

$$\frac{d\bar{\sigma}_{zz}^f}{dz} = -\frac{2\sigma_o^f}{r_o} \tag{8}$$

By assuming that:

$$\frac{\partial \sigma_{zz}^f}{\partial z} = f(z) \tag{9}$$

and using (1b) we have:

$$\frac{\partial \tau_{rz}^f}{\partial r} + f(z) + \frac{\tau_{rz}^f}{r} = 0 \tag{10}$$

This is a first order linear differential equation in terms of τ_{rz}^f which its solution leads to:

$$\tau_{rz}^f = -\frac{1}{2}f(z)\cdot r + \frac{c_1}{r} \tag{11}$$

$\tau_{rz}^f|_{r=0} = 0$ due to symmetry of the cellulose fiber; so we have:

$$\tau_{rz}^f = -\frac{1}{2}f(z)\cdot r \tag{12}$$

Using (11) and (12) we have:

$$c_1 = 0 \tag{13}$$

For simplicity we will represent $\tau_{rz}^f|_{r=r_o}$ byτ_o^f; so we obtain:

$$f(z) = -\frac{2}{r_o}\tau_o^f(z) \tag{14a}$$

$$\tau_{rz}^f = \frac{r}{r_o}\tau_o^f(z) \tag{14b}$$

The boundary condition of (4a) implies that there is no radial normal stress and shear stress on the circumference of the matrix. So we may rewrite Eq. (4a) as:

$$\sigma_{rr}^m|_{r=R} = 0 \tag{15a}$$

$$\tau_{zr}^m|_{r=R} = 0 \tag{15b}$$

In a similar manner rewriting Eq. (5a) leads to:

$$\sigma_{rr}^f|_{-L_f<z<L_f, r=r_o} = \sigma_{rr}^m|_{-L_f<z<L_f, r=r_o} \tag{16a}$$

$$\tau_{zr}^f|_{-L_f<z<L_f, r=r_o} = \tau_{zr}^m|_{-L_f<z<L_f, r=r_o} \tag{16b}$$

Now integrating (1b) with respect to r from r_o to R and using (15b) leads to,

$$\frac{d\bar{\sigma}_{zz}^m}{dz} = \frac{2r_o}{R^2 - r_o^2}\tau_o^f \tag{17}$$

Considering,

$$\bar{\sigma}^m_{zz}(z) = \frac{1}{\pi(R^2 - r_o^2)} \int_{r_o}^{R} \sigma^m_{zz}(r, z) \cdot (2\pi r) \cdot dr \tag{18}$$

then by assuming,

$$\frac{\partial \sigma^m_{zz}}{\partial z} = g(z) \tag{19}$$

were $g(z)$ is an unknown function that must be determined. Inserting (19) in (1b) and integrating with respect to r form r to R leads to:

$$g(z) = \frac{2}{R^2 - r^2} r \cdot \sigma^m_{rz}(r) \;\Rightarrow\; \sigma^m_{rz} = \frac{g(z)}{2} \cdot \frac{R^2 - r^2}{r} \tag{20}$$

Using (20) and (5b),

$$g(z) = \frac{2 \cdot r_o}{R^2 - r_o^2} \tau^f_o \tag{21}$$

Substituting (21) in (20),

$$\tau^m_{rz}(r) = \frac{r_o}{R^2 - r_o^2} \left(\frac{R^2 - r^2}{r} \right) \cdot \tau^f_o \tag{22}$$

and assuming that $|\partial u/\partial z| \prec\prec |\partial w/\partial r|$, i.e., the radial displacement along the radii is much smaller than the axial displacement along the radii, and (2d) and (3d),

$$\tau^f_{rz} = G^f \frac{\partial w^f}{\partial r} \tag{23a}$$

$$\tau^m_{rz} = G^m \frac{\partial w^m}{\partial r} \tag{23b}$$

Using (23b) and (22) we have,

$$\tau^f_o = G^m \frac{R^2 - r_o^2}{R^2 - r^2} \cdot \frac{r}{r_o} \cdot \frac{\partial w^m}{\partial r} \tag{24}$$

Rearranging (24) and integrating from r_o to R leads to,

$$\tau^f_o \int_{r_o}^{R} \left(\frac{R^2}{r} - r \right) dr = \int_{r_o}^{R} G^m \frac{(R^2 - r_o^2)}{r_o} dw^m \;\Rightarrow$$

$$\tau^f_o = G^m \frac{R^2 - r_o^2}{r_o} \frac{w^m_R - w^m_{r_o}}{R^2 \ln(R/r_o) - 1/2(R^2 - r_o^2)} \tag{25}$$

Substitution of (25) into (22) results in,

$$\tau^m_{rz}(r) = G^m \frac{R^2 - r^2}{r} \left[\frac{w^m_R - w^m_{r_o}}{R^2 \ln(R/r_o) - 1/2(R^2 - r_o^2)} \right] \tag{26}$$

Putting (26) into (23b) leads to:

$$\frac{\partial w^m}{\partial r} = \frac{R^2 - r^2}{r} \left[\frac{w^m_R - w^m_{r_o}}{R^2 \ln(R/r_o) - 1/2(R^2 - r_o^2)} \right] \xrightarrow{\int_{r_o}^{r}}$$

$$w^m_r(r, z) = w^m_{r_o} + \left[\frac{(w^m_R - w^m_{r_o}) \cdot (R^2 \ln(r/r_o) - 1/2(r^2 - r_o^2))}{R^2 \ln(R/r_o) - 1/2(R^2 - r_o^2)} \right] \tag{27}$$

Assuming $\sigma_{\theta\theta} + \sigma_{\gamma\gamma} \ll \sigma_{zz}$ for both matrix and the cellulose fiber, due to the fact that we considered the nanocomposite under axial loading, and using (2c), (3c), then we have:

$$\sigma^f_{zz} = E^f \frac{\partial w^f}{\partial z} \tag{28a}$$

$$\sigma^m_{zz} = E^m \frac{\partial w^m}{\partial z} \tag{28b}$$

Substituting (27) into (28b) results in:

$$\sigma^m_{zz} = \sigma^m_{zz}|_{r=r_o} + \frac{R^2 \ln(r/r_o) - 1/2(r^2 - r_o^2)}{R^2 \ln(R/r_o) - 1/2(R^2 - r_o^2)} \times [\sigma^m_{zz}|_{r=R} - \sigma^m_{zz}|_{r=r_o}] \tag{29}$$

Considering the force balance of the composite along the z axis:

$$\pi R^2 \sigma = \int_0^{r_o} \sigma^f_{zz} \cdot (2\pi r)\, dr + \int_{r_o}^{R} \sigma^m_{zz} (2\pi r)\, dr \tag{30}$$

Using (7), (29) and (30) we have:

$$\sigma^m_{zz}|_{r=R} = \sigma^m_{zz}|_{r=r_o} + \frac{(R^2 \ln(R/r_o) - 1/2(R^2 - r_o^2)) \cdot [R^2 \sigma - \bar{\sigma}^f_{zz} r_o^2 + \sigma^m_{zz}|_{r=r_o} (r_o^2 - R^2)]}{R^4 \ln(R/r_o) - 1/4(R^2 - r_o^2) \cdot (3R^2 - r_o^2)} \tag{31}$$

From (8), (25), (28b) and (31) it follows that,

$$\frac{d^2 \overline{\sigma}^f_{zz}}{dz^2} = \frac{R^2 - r_o^2}{r_o^2} \frac{1}{1 + \nu_m} \times \frac{\bar{\sigma}^f_{zz} r_o^2 - R^2 \sigma + \sigma^m_{zz}|_{r_o} (R^2 - r_o^2)}{R^4 \ln(R/r_o) - 1/4(R^2 - r_o^2)(3R^2 - r_o^2)} \tag{32}$$

Assuming that the bounding between the cellulose fiber and matrix to be perfect, i.e., no sliding occurs at the cellulose fiber/matrix interface, we have:

$$\varepsilon^m_{zz}|_{r=r_o} = \varepsilon^f_{zz}|_{r=r_o} \;\Rightarrow\; \sigma^m_z|_{r=r_o} = \frac{E^m}{E^f} \sigma^f_{zz}|_{r=r_o} \tag{33}$$

Assuming low volume fraction of the cellulose fiber,

$$\sigma^f_{zz} \approx \bar{\sigma}^f_{zz} \tag{34}$$

and using (34) and (32) we have:

$$\frac{d^2 \bar{\sigma}^f_{zz}}{dz^2} = \frac{R^2 - r_o^2}{r_o^2} \frac{1}{1 + \nu_m} \times \frac{\bar{\sigma}^f_{zz} [r_o^2 + (E^m/E^f)(R^2 - r_o^2)] - R^2 \sigma}{R^4 \ln(R/r_o) - 1/4(R^2 - r_o^2)(3R^2 - r_o^2)} \tag{35}$$

By considering η as,

$$\eta = -\frac{R^2 - r_o^2}{r_o^2} \frac{1}{1 + \nu_m} \times \frac{1}{R^4 \ln(R/r_o) - 1/4(R^2 - r_o^2)(3R^2 - r_o^2)} \tag{36}$$

RESEARCH ARTICLE

Equation (35) becomes:

$$\frac{d^2\bar{\sigma}_{zz}^f}{dz^2}+\eta\left[r_o^2+\frac{E^m}{E^f}(R^2-r_o^2)\right]\bar{\sigma}_{zz}^f=R^2\eta\sigma \tag{37}$$

Equation (37) represents an ordinary differential equation with constant coefficients and has a solution as:

$$\begin{aligned}\bar{\sigma}_{zz}^f=&A\cdot\sinh\left(\sqrt{-\eta\left[r_o^2+\frac{E^m}{E^f}(R^2-r_o^2)\right]}z\right)\\&+B\cdot\cosh\left(\sqrt{-\eta\left[r_o^2+\frac{E^m}{E^f}(R^2-r_o^2)\right]}z\right)\\&-\frac{R^2\sigma}{r_o^2+(E^m/E^f)(R^2-r_o^2)}\end{aligned} \tag{38}$$

Substituting (38) into (8) results in,

$$\begin{aligned}\bar{\sigma}_{zz}^f=&A\cdot\sqrt{-\eta\left[r_o^2+\frac{E^m}{E^f}(R^2-r_o^2)\right]}\\&\cdot\cosh\left(\sqrt{-\eta\left[r_o^2+\frac{E^m}{E^f}(R^2-r_o^2)\right]}z\right)\\&+B\cdot\sqrt{-\eta\left[r_o^2+\frac{E^m}{E^f}(R^2-r_o^2)\right]}\\&\cdot\sinh\left(\sqrt{-\eta\left[r_o^2+\frac{E^m}{E^f}(R^2-r_o^2)\right]}z\right)=-\frac{2\sigma_o^f}{r_o}\end{aligned} \tag{39}$$

Equation (39) can be rewriting in the following form as:

$$\frac{2\sigma_o^f}{r_o}=\frac{1}{2}\cdot r_o\cdot\alpha\cdot[A\cdot\cosh(\alpha\cdot z)+B\cdot\sinh(\alpha\cdot z)] \tag{40}$$

in which α is,

$$\alpha=\sqrt{-\eta\left[r_o^2+\frac{E^m}{E^f}(R^2-r_o^2)\right]} \tag{41}$$

Using (31), (33), (34) and (38) in (29) result in,

$$\begin{aligned}\sigma_{zz}^f=&\frac{R^2\ln(r/r_o)-1/2(r^2-r_o^2)}{R^2\ln(R/r_o)-1/4(R^2-r_o^2)\cdot(3R^2-r_o^2)}R^2\sigma\\&+\left\{\frac{E^m}{E^f}-\frac{[R^2\ln(R/r_o)-1/2(R^2-r_o^2)]\cdot[r_o^2+(E^m/E^f)(R^2-r_o^2)]}{R^4\ln(R/r_o)-1/4(R^2-r_o^2)\cdot(3R^2-r_o^2)}\right\}\\&\times\left[A\cdot\sinh(\alpha\cdot z)+B\cdot\cosh(\alpha\cdot z)\right.\\&\left.+\frac{R^2\sigma}{[r_o^2+(E^m/E^f)(R^2-r_o^2)]}\right]\end{aligned} \tag{42}$$

Using (40) in (14b) results in,

$$\sigma_{rz}^f=-\frac{r}{2}\{A\cdot\alpha\cdot\cosh(\alpha\cdot z)+B\cdot\alpha\cdot\sinh(\alpha\cdot z)\} \tag{43}$$

Finally, the use of (40) in (22) gives

$$\begin{aligned}\sigma_{rz}^m=&\frac{r_o^2}{2(R^2-r_o^2)}\left(r-\frac{R^2}{r}\right)\\&\times\{A\cdot\alpha\cdot\cosh(\alpha\cdot z)+B\cdot\alpha\cdot\sinh(\alpha\cdot z)\}\end{aligned} \tag{44}$$

Equations (38), (40) and (42) to (44) represent some expressions for unknown stresses of $\bar{\sigma}_{zz}^f, \sigma_{rz}^f, \sigma_{zz}^m$ and σ_{rz}^m. To calculate the value of two constant coefficients A and B, the pure matrix region must be considered. That is a matrix with an embedded virtual solid cellulose fiber with outer radius equal to the outer radius of the actual cellulose fiber in the reinforced region.

3.2. Solution in Pure Matrix Region

Equation (38) for this region of the RVE would be as follows:

$$\begin{aligned}&\bar{\sigma}_{zz}^m=\\&A'\cdot\sinh\left(\sqrt{\frac{R^2-r_o^2}{r_o^2}\frac{1}{1+\nu_m}\frac{R^2}{R^4\ln(R/r_o)-1/4(R^2-r_o^2)(3R^2-r_o^2)}}z\right)\\&+B'\cdot\cosh\left(\sqrt{\frac{R^2-r_o^2}{r_o^2}\frac{1}{1+\nu_m}\frac{R^2}{R^4\ln(R/r_o)-1/4(R^2-r_o^2)(3R^2-r_o^2)}}z\right)\\&+\sigma\end{aligned} \tag{45}$$

A' and B' are constants, the same as A and B in (38) but in the pure matrix region. By substituting (45) into (8) and the consequent result into (14b) one would obtain:

$$\sigma_{rz}^{fm}=-\frac{r}{2}(A'\cdot\beta\cdot\cosh(\beta\cdot z)+B'\cdot\beta\cdot\sinh(\beta\cdot z)) \tag{46}$$

in which:

$$\beta=\sqrt{\frac{R^2-r_o^2}{r_o^2}\frac{1}{1+\nu_m}\frac{R^2}{R^4\ln(R/r_o)-1/4(R^2-r_o^2)(3R^2-r_o^2)}} \tag{47}$$

In order to calculate the unknown coefficients A' and B' we will apply the boundary conditions which are listed in (4b) and (5b). After some calculations, A' and B' will be obtained as follows:

$$A'=0 \tag{48a}$$

$$B'=\frac{\sigma}{\cosh(\alpha\cdot L_f)}\left[1-\frac{R^2}{r_o^2+(E^m/E^f)(R^2-r_o^2)}\right] \tag{48b}$$

Substituting the values of A' and B' in Eqs. (38), (40) and (42–44), the following relations are obtained:

$$\begin{aligned}\bar{\sigma}_{zz}^f=&\sigma\left(1-\frac{R^2}{r_o^2+(E^m/E^f)(R^2-r_o^2)}\right)\frac{\cosh(\alpha\cdot z)}{\cosh(\alpha\cdot L_f)}\\&+\frac{\sigma R^2}{r_o^2+(E^m/E^f)(R^2-r_o^2)}\end{aligned} \tag{49a}$$

RESEARCH ARTICLE

$$\sigma_{rz}^{f}|_{r=r_o} = \frac{r_o}{2}\left[\frac{\alpha}{\cosh(\alpha\cdot L_f)}\left(\frac{R^2}{r_o^2+(E^m/E^f)(R^2-r_o^2)}-1\right)\cdot\sinh(\alpha\cdot z)\right]\cdot\sigma \quad (49b)$$

$$\sigma_{zz}^{m} = \frac{R^2\ln(r/r_o)-1/2(r^2-r_o^2)}{R^4\ln(R/r_o)-1/4(R^2-r_o^2)\cdot(3R^2-r_o^2)}R^2\sigma + \left\{\frac{E^m}{E^f}-\frac{[R^2\ln(R/r_o)-1/2(R^2-r_o^2)]\cdot[r_o^2+(E^m/E^f)(R^2-r_o^2)]}{R^4\ln(R/r_o)-1/4(R^2-r_o^2)\cdot(3R^2-r_o^2)}\right\} \times\left[\frac{\cosh(\alpha\cdot z)}{\cosh(\alpha\cdot L_f)}\left(1-\frac{R^2}{r_o^2+(E^m/E^f)(R^2-r_o^2)}\right)+\frac{R^2}{[r_o^2+(E^m/E^f)(R^2-r_o^2)]}\right]\cdot\sigma \quad (49c)$$

$$\sigma_{rz}^{f} = \frac{r}{2}\left[\frac{\alpha\cdot\sinh(\alpha\cdot z)}{\cosh(\alpha\cdot L_f)}\left(\frac{R^2}{r_o^2+(E^m/E^f)(R^2-r_o^2)}-1\right)\right]\cdot\sigma \quad (49d)$$

$$\sigma_{rz}^{m} = \frac{r_o^2}{2(R^2-r_o^2)}\left(r-\frac{R^2}{r}\right) \times\left[\frac{\alpha\cdot\sinh(\alpha\cdot z)}{\cosh(\alpha\cdot L_f)}\left(1-\frac{R^2}{r_o^2+(E^m/E^f)(R^2-r_o^2)}\right)\right]\cdot\sigma \quad (49e)$$

In the following section a numerical example has been provided, to show the configuration of the stress on the cellulose fiber and on the interface between the cellulose fiber/matrix.

4. NUMERICAL SOLUTION AND CASE STUDY

Based on the derived relations for a cellulose fiber placed in the epoxy matrix and subjected to an axial constant traction, the shear stress distribution in the medium was calculated. In this study the mean axial stress of the fiber and shear stress distribution along the fiber/matrix interface were plotted for three fibers with different aspect ratios. The epoxy matrix considered to have the following properties, $E_m = 2.41$ GPa and $\nu_m = 0.35$.[23] Also to fulfill the assumption of low fiber concentration, we have considered $R = 5\cdot r_o$.

As it was discussed earlier, there are many sources for producing cellulose fibers which result in variation in mechanical and geometrical properties of cellulose nanofibers. While with cellulose fibers which are produced from cotton the diameter of about 10 nm and length of about 300 nm has been reported in the literature, for cellulose fibers originated from tunicate the average diameter of 10 nm and length of 2000 nm is reported.[16, 24] Different tensile strength and Young's modulus are also reported for cellulose fibers with different origins. For example while

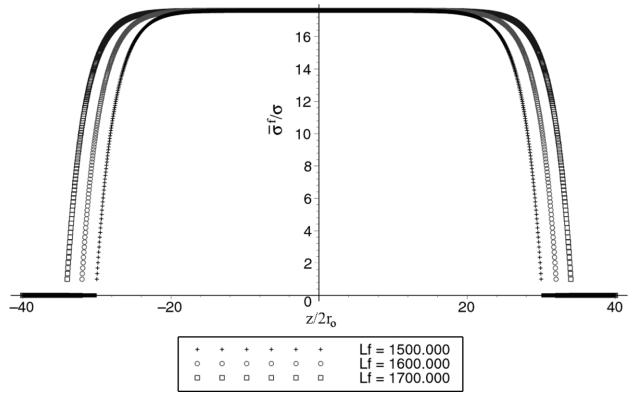

Fig. 3. Distribution of dimensionless mean axial stress, $\bar{\sigma}^f$, versus axial position of cellulose fiber which is made dimensionless by its diameter.

tensile strength and Young's modulus are about 600 MPa and 15 GPa for Sisal, respectively; they are 175 MPa and 5 GPa for Coir[25] which are microfibers. Also for bacterial cellulose, Young's modulus of about 140 MPa and 80 GPa are reported in the previous research studies.[26] In a recent study, Raman spectroscopy was used to measure the elastic modulus of cotton-based and bacterial-based cellulose nanocrystals embedded in epoxy matrix. Hsieh et al.[27] obtained a value of 114 GPa for the elastic modulus of bacterial cellulose nanofibers and Rusil et al.[28] found an upper value of 105 GPa and a lower value of 57 GPa for the elastic modulus of cotton cellulose nanofibers. Both of the reported values for cotton cellulose nanofibers are lower than the earlier data published in the literature. This may be due to the smaller aspect ratio in cotton-based cellulose nanofibers compare to other sources, however the underlying mechanisms have not been explored.

In the current work, three fibers with the same diameter but different lengths were considered. The fibers of interest have the following properties: $r_o = 25$ nm; $2L_f = 1500$ nm, 1600 nm and 1700 nm; $E_f = 138$ GPa.[26, 29] The mean stress is shown in Figure 3 and the shear stress between the cellulose fiber/matrix interface is shown in Figure 4. It can be seen that the axial stress grows rapidly at the beginning, then it continue growing very slowly till it reaches its

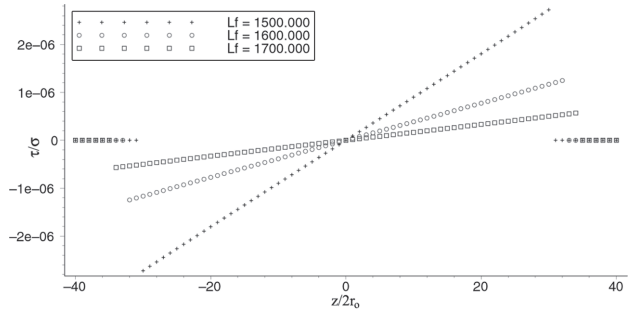

Fig. 4. Dimensionless shear stress distribution versus length of cellulose fiber, on the interface of fiber/matrix.

RESEARCH ARTICLE

maximum at the middle of the fiber. According to graph, the maximum axial stress is not affected significantly by increasing the aspect ratio. Therefore, if axial stress determines the failure of the fiber, then using fibers with aspect ratios greater than a critical value is not admissible. We may define a critical value for the fibers as the minimum aspect ratio that the greatest mean stress in the fiber gets to its maximum value.

It also has been shown that the maximum shear stress occurs at the extreme ends of the fiber. Therefore fiber matrix debonding may occur at the extreme ends which lead to composite failure. A conclusion that we can obtain is that fibers with higher aspect ratios, have higher loading capability. It is due to the fact that the maximum shear stress is lower for the longer fibers compared to the shorter ones. Therefore it can be concluded that fibers with higher aspect ratios can carry more load before failure.

The obtained results are comparable to the results which have been reported for other materials such as carbon nanotubes.[30, 31] The calculated stress distribution on the cellulose nanofibers is quit similar to the one obtained for CNT even when the effect of stress transfer from the fiber ends were neglected.[30] This is due to the fact that the stress transfer from the ends of the CNT is negligible compared to the stress transfer via the side walls. By considering the stress transfer via the fiber ends we make the calculations valid for the case of short fibers which is the case for the nano fibers. This resulted in smoother transition of stress distribution at the interface of nanofiber and matrix, while others reported a sharp transition in the value of stress at the interface.[23]

5. CONCLUSION

In this work a rigorous mathematical framework to model the stress distribution at the interface of a cellulose fiber and composite matrix was derived. Our results indicated that the ability of the cellulose fiber to stress transfer can be improved by increasing the aspect ratio of the fiber which is defined as the ratio of its length to its diameter. The shear stress transfer can also increase by increasing the aspect ratio of cellulose fibers. Furthermore, axial stress reaches to the maximum value at the center of the fiber while shear stress has the maximum value at the fiber surface and vanishes at the middle. On the other hand, it has been shown that while a non-linear relationship exists between the shear stress and the applied axial stress, but for the practical fiber lengths it well fits a linear function.

NOMENCLATURE

z	Axial coordinate of the RVE[a]
r	Radial coordinate of the RVE
R	Radius of the RVE
r_o	Outer radius of the cellulose fiber
t	Thickness of cellulose fiber's wall
ε	Strain
σ	Constant applied axial stress to the RVE
$\bar{\sigma}$	Average axial normal stress
τ	Shear Stress
ν	Poisson's ratio
G	Shear Modulus
γ	Shear strain
m	Parameters associated to matrix material
f	Parameters associated to cellulose fiber
u	Radial displacement
w	Axial displacement
T	Traction
L	Length of the RVE

[a]Representative Volume Element

Acknowledgments: We appreciate the Michigan Technological University for providing the financial support.

References

1. S. Beck-Candanedo, M. Roman, and D. G. Gray, 6, 1048 **(2005)**.
2. L. Chazeau, J. Y. Cavaillé, and P. Terech, *Polymer* 40, 5333 **(1999)**.
3. A. N. Nakagaito, S. Iwamoto, and H. Yano, *Appl. Phys. A: Mater. Sci. Process.* 80, 93 **(2005)**; A. K. Bledzki and J. Gassan, *Prog. Polym. Sci.* 24, 221 **(1999)**.
4. J. F. Beecher, *Nat Nano* 2, 466 **(2007)**.
5. J. Y. Cavaillé, A. Dufresne, and W. Helbert, 17, 604 **(1996)**; J. Y. Cavaillé, E. Chabert, L. Chazeau, R. Dendievel, L. Flandin, C. Gauthier, and Y. Bréchet, 3, 571 **(2001)**.
6. A. Bhatnagar and M. Sain, 24, 1259 **(2005)**; H. Yano and S. Nakahara, *Journal of Materials Science* 39, 1635 **(2004)**; Y. Pu, J. Zhang, T. Elder et al., *Composites Part B: Engineering* 38, 360 **(2007)**; M. Roohani, Y. Habibi, N. M. Belgacem et al., *Eur. Polym. J.* 44, 2489 **(2008)**; M. A. S. Azizi Samir, L. Chazeau, F. Alloin et al., *Electrochim. Acta* 50, 3897 **(2005)**.
7. Y. Z. Wan, Y. Huang, C. D. Yuan et al., *Mater. Sci. Eng., C* 27, 855 **(2007)**.
8. M. A. S. AziziSamir, F. Alloin, and A. Dufresne, 6, 612 **(2005)**; X. Cao, H. Dong, and C. M. Li, 8, 899 **(2007)**; N. E. Marcovich, M. L. Auad, N. E. Bellesi et al., *J. Mater. Res.* 21, 870 **(2006)**; I. Kvien, J. Sugiyama, M. Votrubec et al., *J. Mater. Sci.* 42, 8163 **(2007)**.
9. V. Lapa, J. M. Suarez, L. Visconte et al., *J. Mater. Sci.* 42, 9934 **(2007)**.
10. Y. J. Choi and J. Simonsen, *J. Nanosci. Nanotechnol.* 6, 633 **(2006)**.
11. M. Auad, L. A. Vasili, S. Contos et al., *Polym. Int.* 57, 651 **(2008)**.
12. S. Noorani, J. Simonsen, and S. Atre, *Cellulose* 14, 577 **(2007)**.
13. T. Zimmermann, E. Pöhler, and T. Geiger, 6, 754 **(2004)**.
14. T. Zimmermann, E. Pöhler, and P. Schwaller, 7, 1156 **(2005)**.
15. A. K. Mohanty, M. Misra, and L. T. Drzal, Natural Fibers, Biopolymers, and Biocomposites, Taylor & Francis/CRC Press, Boca Raton, FL **(2005)**; W. Helbert, J. Y. Cavaillé, and A. Dufresne, 17, 604 **(1996)**; P. Hajji, J. Y. Cavaillé, V. Favier et al., 17, 612 **(1996)**.
16. V. Favier, H. Chanzy, and J. Y. Cavaille, 28, 6365 **(1995)**; A. Dufresne, M. B. Kellerhals, and B. Witholt, 32, 7396 **(1999)**.
17. J. F. Graham, C. McCague, O. L. Warren et al., *Polymer* 41, 4761 **(2000)**; M. R. VanLandingham, J. S. Villarrubia, W. F. Guthrie et al., 167, 15 **(2001)**; L. Drzal, *Epoxy Resins and Composites II* 1 **(1986)**; J.-K. Kim and Y. W. Mai, Engineered Interfaces in Fiber Reinforced Composites, 1st edn., Elsevier Sciences, Amsterdam, New York

RESEARCH ARTICLE

(1998); J. G. Williams, M. E. Donnellan, M. R. James et al., *Mater. Sci. Eng., A* 126, 305 **(1990)**; M. R. Piggot, Presented at the *Materials Research Society Symposium*, 1990 (unpublished).
18. S.-H. Lee, S. Wang, G. M. Pharr et al., *Composites Part A: Applied Science and Manufacturing* 38, 1517 **(2007)**.
19. D. Qian, W. K. Liu, and R. S. Ruoff, *Compos. Sci. Technol.* 63, 1561 **(2003)**.
20. A. K. Mohanty, M. Misra, and L. T. Drzal, *Compos. Interfaces* 8, 313 **(2001)**.
21. M. Bengtsson, P. Gatenholm, and K. Oksman, *Compos. Sci. Technol.* 65, 1468 **(2005)**.
22. A. P. Boresi and K. P. Chong, Elasticity in Engineering Mechanics, Wiley, New York **(2000)**, Vol. 4.
23. W. D. Callister, Materials Science and Engineering : An Introduction, 6th edn., Wiley, New York **(2003)**.
24. M. M. de Souza Lima and R. Borsali, 18, 992 **(2002)**.
25. S. J. Eichhorn, C. A. Baillie, N. Zafeiropoulos et al., *J. Mater. Sci.* 36, 2107 **(2001)**.
26. G. Guhados, W. Wan, and J. L. Hutter, 21, 6642 **(2005)**; H. Yano, J. Sugiyama, A. N. Nakagaito et al., 17, 153 **(2005)**.
27. Y. C. Hsieh, H. Yano, M. Nogi et al., *Cellulose* 15, 507 **(2008)**.
28. R. Rusli and S. J. Eichhorn, *Appl. Phys. Lett.* 93, 033111 **(2008)**.
29. Y. Z. Wan, L. Hong, S. R. Jia et al., *Compos. Sci. Technol.* 66, 1825 **(2006)**.
30. A. Haque and A. Ramasetty, *Compos. Struct.* 71, 68 **(2005)**.
31. N. Hu, H. Fukunaga, C. Lu et al., *Proceedings of the Royal Society A: Mathematical, Physical and Engineering Sciences* 461 1685 **(2005)**; W. Wang, P. Ciselli, E. Kuznetsov et al., *Philosophical Transactions of the Royal Society A: Mathematical, Physical and Engineering Sciences* 366 1613 **(2008)**.

Received: 1 December 2008. Accepted: 8 January 2009.

RESEARCH ARTICLE